

## **Review of “Physical Processes in Carbon Storage” by Udo Weyer**

Reviewed by E.O. Frind and J.W. Molson  
January 11, 2010

We have briefly reviewed this paper consisting of 7 chapters plus a slide show, focusing on the text portion. The main thrust of the paper is that there exists a physical process the author chooses to give the term “buoyancy reversal”, and that this process can be used to advantage in the sequestration of CO<sub>2</sub> in geologic formations. In addition, the author has identified a number of deficiencies in conventional subsurface modelling techniques.

Our review shows that buoyancy reversal exists, although we might choose a slightly different term to describe this phenomenon. This phenomenon is a natural physical process, and the conditions under which it occurs can be readily predicted. Any groundwater model based on sound fundamental theories should be able to predict buoyancy reversal under the appropriate conditions.

With regard to modelling deficiencies, we are confident that standard techniques used in hydrogeology, at least as far as models originated and developed at the University of Waterloo are concerned, are sound. The development of groundwater models at Waterloo started under the direction of the first reviewer in the 1970s, initially in close cooperation with George Pinder at Princeton University. Our models are based on, and are consistent with, the fundamental theories postulated by Hubbert (1940).

We cannot comment on the validity of reservoir simulation models used in the oil industry. However, on the basis of the evidence presented by the author, we agree that certain reservoir simulation models may have deficiencies which would make them unsuitable for application to groundwater systems, including CO<sub>2</sub> sequestration.

### **Detailed Comments**

#### ***Chapter 2***

The well-known figures in this chapter form the basis of current groundwater flow theory as taught at many universities. The conclusions drawn in the chapter are, of course, correct, but they are not new. On page 9, the statement that geologic layers are homogeneous and isotropic in mathematical models should not be generalized because UW models, as well as many other models we are familiar with, allow heterogeneity and anisotropy within layers as a standard feature. Further, the finding that there is twice as much water flowing in the aquitard should not be generalized either. This is undoubtedly true for the case considered here because some water flowing in the aquitard never makes it to the aquifer; in general, however, how much water will flow where will depend on the proportions of the various members of the system, the driving forces, and the boundary conditions.

We feel that the author may be struggling against the old-school thinking that considers hydrogeology in terms of aquifers and aquitards. A better way is to think 3D flow systems.

### **Chapter 3**

One focal idea in this chapter is that a flow system can be represented by means of relative permeabilities (called “contrast permeabilities” by the author). It can be shown easily that this approach is valid, provided the flow is steady state. In that case, the flow system is governed by the Darcy equation. Since there is no change in storage involved, the fluid mass continuity equation is redundant. The Darcy equation is

$$q = -K\nabla h$$

where  $q$  is the flux,  $K$  is the hydraulic conductivity, and  $h$  is the hydraulic head. If the flow system is at steady state,  $\nabla h$  will be constant in time everywhere (but variable in space if the system is heterogeneous). So we can say

$$\nabla h = -q / K$$

for every point in the system. This means that we can multiply the  $K$ -field by any constant, provided we do the same to  $q$ , and the flow system will stay the same.

P. 11, last line: “principle flow patterns” should be “principal flow patterns”  
principle: noun, denoting some standard or fundamental truth  
principal: adjective, denoting first among a group

Fig. 2: See also papers by Frind and Matanga (1985) and Frind et al. (1985), showing the dual theory for potentials and streamfunctions.

P. 13: The finding that “variable density flow can be modelled with fresh water flow models” should not be generalized. In the classical seawater intrusion problem, the seawater will sink and will form a wedge under the freshwater; so the density difference will control the flow. See the two papers by Frind (1982). In the equally classical salt dome problem, water with similar density will rise. So whether the water will sink or rise will depend on the dynamics of the system.

Bottom of p. 14: This paragraph ends with a question that has an obvious answer readily apparent from the figure. See my comments on Chapter 2. Think flow systems.

P. 15 bottom: Again, think flow systems. The flow in the aquifer can only be approximately normal to the flow in the aquitard, as long as some flow crosses the interface.

Conclusions for Ch. 3:

1. True, but not new.
2. Applicability to variable density flow should be checked.

3. As noted above, whether salt water with a density of 1.03 rises or sinks depends on the flow system. We have no doubt that the author's observations are correct. But this observation cannot be generalized. The flow direction will always depend on the vector sum of the driving forces, of which the body force is only one.

4. True only for specific cases, and cannot be generalized. The converse, namely that more water flows in the aquifer than in the aquitard, can also be true for specific cases. Overall, in my view, the question is not very relevant, and I would avoid statements of this sort. Again, think flow systems.

### Chapter 4

The first line in paragraph 2 states as a general assumption (subsequently to be criticized by the author) that hydrocarbons and CO<sub>2</sub> will rise vertically upward and heavier fluids will sink to the bottom. Again, we would caution against generalizing this statement. For example, models developed at Waterloo do not use this assumption, and we are not aware of other groundwater models that do.

A brief check of the most fundamental theories underlying our models, which are generally based on the theories of Hubbert (1940), Bear (1972), and Freeze and Cherry (1979), shows the following (for the case of constant fluid density):

1. Potential energy: The potential energy of a fluid mass is the work done per unit fluid mass, and it is the sum of gravitational potential and pressure potential (inertial potential is neglected):

$$\phi = \phi_g + \phi_p = g(z - z_0) + \frac{(p - p_0)}{\rho} \quad (\text{L}^2/\text{T}^2)$$

Or, letting  $z_0 = 0$  and  $p_0 = 0$ :

$$h = \frac{\phi}{g} = z + \frac{p}{\rho g} \quad (\text{L})$$

2. Darcy equation: The Darcy equation expresses the fluid flux in terms of the basic properties of the medium (permeability  $k$ ), the fluid (viscosity  $\mu$ ), and the driving force per unit volume of the fluid ( $\rho g dh/dL$ ):

$$q = -k \frac{1}{\mu} \rho g \frac{dh}{dL} \quad (\text{L}/\text{T})$$

3. Continuity equation (Darcy equation embedded, written in terms of head):

$$\text{fluid mass into a control volume} - \text{fluid mass out} = \text{change in storage}$$

The above shows that potentials are expressed per unit mass, while the Darcy flux (an experimental quantity) and the continuity equation are expressed per unit volume. This creates

no inconsistency as long as the fluid density is constant. The same holds for the model that was developed to generate flownets (Frind and Matanga, 1985), where both the potential and the streamfunction equations are developed on a per-volume basis. In all models, vector quantities are written in terms of 3D Cartesian components.

For the variable density case, as in the case of seawater intrusion, the continuity equation is initially written in terms of pressure and then reformulated in terms of equivalent freshwater head, which yields a body force term. The body force term expresses the force of gravity on a parcel of fluid. If the density of the parcel is higher than that of the surrounding fluid, the body force will act downward; if it is lighter, it will act upward. But this does not mean that the fluid parcel will necessarily move down or up, it just means that there will be a force component acting in that direction.

The equivalent freshwater head approach, first developed by Frind (1982), has since become standard. We have also developed multiphase models (see two papers by Kueper and Frind, 1991) for the flow of dense non-aqueous liquids (DNAPLs) and light non-aqueous liquids (LNAPLs). These models were deliberately developed from basic principles, without borrowing from reservoir models that were already in existence at the time.

To show that buoyancy reversal can be obtained easily without a sophisticated model, we have done some numerical experiments, which are described below. The results show that a reversal of the pressure gradient can occur naturally across a low- $K$  layer, provided a downward flux of sufficient magnitude exists. Since neither density nor buoyancy play a role in these calculations, we believe that the term “pressure gradient reversal” is more appropriate than “buoyancy reversal” to describe this phenomenon.

It should be noted that for systems involving fluids of variable density, the results may be different. Such cases should be further investigated.

Conclusion 2 for Chapter 4 presents buoyancy reversal as an additional line of defense against CO<sub>2</sub> leakage. In our view, this statement, as placed in the text, is premature. By itself, buoyancy reversal cannot be seen as a line of defense because this phenomenon depends on the pressure, which will change in the course of CO<sub>2</sub> injection. However, the author’s intention becomes clearer in the next chapter, where he proposes to pump water into the overlying layer to balance the increased pressure of the CO<sub>2</sub>.

## *Chapter 5*

This chapter starts by introducing the basic equations for the mechanical groundwater force field, including gravitational, pressure, and capillary forces. We should note that these equations also form the basis of the multiphase flow models we are familiar with.

We would agree that reservoir simulators that take the caprock as the top model boundary are unsuitable for the modelling of CO<sub>2</sub> sequestration. On the other hand, a multiphase model such as the one by Kueper and Frind (1991), which has been developed to simulate the dynamic

advance of a non-aqueous phase into a heterogeneous groundwater system, would satisfy the criteria stated by Chadwick et al. (2009), as quoted by the author.

In this chapter, the author discusses the dynamics of an oil reservoir undergoing first enhanced oil recovery, followed by CO<sub>2</sub> injection. He shows that the advantage of buoyancy reversal would be potentially eradicated due the increased pressure, but that this effect could be counteracted by injecting water above the caprock. The discussion is generally in qualitative terms. This interesting idea should be tested and developed further by applying an advanced multiphase flow model. Appropriate simulations would provide insights into various critical issues such as the duration of pumping required, the long-term effectiveness of the method in sequestering the CO<sub>2</sub>, and the economics of the scheme.

## ***Chapter 6***

This chapter defines the conditions for buoyancy reversal. As we will show below in our numerical experiments, these conditions are valid. In somewhat briefer form (see Fig. 3, Case 3 below), the threshold conditions for buoyancy (pressure gradient) reversal in an aquitard (fresh water at any constant temperature) can be stated as:

Pressure gradient in aquitard = zero  
Hydraulic gradient over the aquitard = -1 (gravity flow)  
Fluid force = gravitational force  $g$   
Downward flux  $q$  = hydraulic conductivity  $K$  of aquitard (both in consistent units)

Checking out Fig. 1 in Ch. 6 of the author's papers, there seems to be some discrepancy. The flux (y-axis) is given in m/s, so the values should agree with the  $K$ -values in m/s given along the top horizontal axis. However, there is a two-order-of-magnitude difference. This should be checked. The error may be in the labelling of the horizontal axis.

In Fig. 2, the flux in m/s (vertical axis) corresponds with the values of  $K$  in m/s (top axis) for the line labelled  $\nabla\phi = 9.81 \text{ m/s}^2$ . So this figure is correct. Since this figure is based on actual field data, it shows that the theoretical threshold value of  $q = K$  can vary under field conditions. The deviation from the theoretical threshold value seems to be about one order of magnitude. A likely source of error of this magnitude may be the heterogeneity of the aquifer material, and measurement errors arising from that heterogeneity. Density differences could not account for the difference.

With respect to ease of use, this figure could be made more understandable by using consistent units. The jumble of different units at the bottom of p. 29 is not helpful.

P. 29 line 3: change "removal" to "reversal".

## ***Chapter 7***

We generally agree with the objectives laid out in this chapter, but we are concerned about some of the details. We have little experience with off-shore oil fields, but we feel it would be risky to

assume that the flow system in such a flow field is hydrostatic. It may be so initially, but I would expect that extracting oil will change this condition. In my opinion, any interference into the subsurface should be handled by assuming dynamic conditions. There is no plausible reason to do otherwise. State-of-the-art models are based on the assumption of dynamic conditions in any case.

We disagree with the statement in par. 3 on p. 35, which states that “present fluid flow programs in hydrogeology ... assume the buoyancy of hydrostatic conditions.” This may be true for reservoir simulators, but certainly not for groundwater models. Likewise, the statement that fluid flow models are based on the assumption of “ $\nabla p$  as the driving force for fluid flow” is not true, as we have shown above. As far as we are aware, the basic driving force in standard groundwater models is always the hydraulic gradient  $\nabla h$ . Other driving forces may be added as the situation demands, such as the body force for density dependent flow including thermal situations (as discussed above), or capillary forces for multiphase flow.

## Numerical Experiments

### *1D Column*

We start with a simple spreadsheet analysis to simulate vertical downward flow in a 1D column consisting of 3 layers. This case is similar to the case show in Fig. 7 in Ch. 4 of the author’s papers. The middle layer is the aquitard, which has a lower value of  $K$ . Three cases, which differ only in the value of  $K_{\text{aquitard}}$ , are considered.

We make use of the fundamental fact (Bear 1972) that the flow system obtained by means of the harmonic mean  $K$  (valid for series flow) is identical to the flow system corresponding to the actual  $K$  of the layers. With the harmonic mean  $K$  and the gradient, the flux can be calculated. The flux is continuous across the layers. Then, using the flux and the hydraulic conductivity of each layer, the head drop across each layer can be calculated. Starting at the top and proceeding downward, adding the drops over each layer gives the hydraulic head at each interface. Finally, the corresponding pressure head is obtained by subtracting the elevation. A “buoyancy force” does not appear explicitly in the calculations, nor is it necessary since the density is constant.

The results of the analysis are given in Figures 1 to 3. The key findings are as follows:

Figure 1, Case 1: Homogeneous material (all 3 layers have the same  $K$ ). Pressure increases uniformly with depth.

Figure 2, Case 2: The middle layer (aquitard) has a lower  $K$  by 2 orders of magnitude relative to that of the aquifers. From the top down, pressure increases in the upper layer, then decreases in the middle layer, then increases again in the lower layer. Consequently, the pressure gradient reverses within the low- $K$  layer.

Figure 3, Case 3: Critical (threshold) case with respect to pressure gradient reversal. The flux  $q$  is such that pressure stays constant within the middle layer, the pressure gradient is zero, the

hydraulic gradient  $\nabla h = -1$  (gravity flow), and consequently the fluid force = gravitational force  $g$ . This occurs when the downward flux exactly equals the hydraulic conductivity of the middle layer (compare values in table).

### ***2D Hubbert-type Cross-sectional Flow System***

Here we use the model FLONET to simulate 2D flow in a cross-section consisting of a watertable aquifer, an aquitard, and a lower confined aquifer. In terms of Hubbert-type flow, the section will represent either a complete flow system from recharge area to discharge area, or one half of such a system. The  $K$ -values of the units vary.

Figure 4: Half flow system, specified recharge,  $K_{\text{aquitard}}/K_{\text{aquifer}} = 10^{-2}$  to  $10^{-5}$ . The boundary condition at the left is a symmetry boundary, at the right a specified head, and a constant recharge is specified across the top. The first column of plots on the left shows the streamfunctions, the second column the pressure head, and the third the pressure head profiles.  $K_{\text{aquitard}}$  decreases downward in the figure. With a two-order-of-magnitude  $K$ -contrast (top plot), the flow still penetrates into the lower aquifer, but as  $K_{\text{aquitard}}$  decreases, flow becomes increasingly confined to the top aquifer. There is only a slight effect on the pressure profile, and no reversal of the pressure gradient occurs. This example shows that there must be enough flow across the aquitard for pressure gradient reversal to occur.

Figure 5: Same as Fig. 4, except that the head for the lower aquifer at the right boundary decreases as the  $K$  of the aquitard decreases, thus drawing more flow into the lower aquifer. Although most of the flow is still in the top aquifer, enough flow crosses the aquitard to cause an increasing reversal of the pressure gradient with depth as  $K_{\text{aquitard}}$  decreases.

Figure 6: Here we use a full Hubbert-type cross-section from recharge area to discharge area. The lateral boundaries are symmetry boundaries and the top has a specified head. The aquitard has a 2 order-of-magnitude lower  $K$  than the upper aquifer, while the lower aquifer has a  $K$  that increases from  $10^{-7}$  to  $10^{-2}$  going down the figure. The effect of this  $K$ -increase is to draw more water into the lower aquifer, so that flow across the aquitard is maintained. The profile plots at the right of the figure show two profiles, one in the recharge area and one in the discharge area. The pressure gradient in the recharge area is seen to reverse, while that in the discharge area tends to flatten out.

Figure 7: This figure shows a more complete representation of the pressure profile across the full flow system from recharge area to discharge area. The system consists of an upper aquifer with  $K = 10^{-7}$ , underlain by an aquitard with  $K = 10^{-9}$ , again underlain by a highly permeable aquifer with  $K = 10^{-2}$ . With this configuration, a large part of the flow passes through the aquitard and the lower aquifer. The pressure gradient reverses in the recharge area (left part of figure), with the reversal decreasing toward the centre of the system. In the discharge area, the profile increasingly flattens out. This example shows clearly that pressure gradient reversal can only occur in a groundwater recharge area.

The above examples demonstrate the conditions under which pressure gradient reversal can be obtained within natural flow systems. They are not intended to identify areas suitable for CO<sub>2</sub> sequestration. More on this below.

## **Discussion and Conclusions**

Our numerical experiments show that under conditions of downward flow across an aquitard, the pressure gradient can reverse, causing the pressure to decrease in the downward direction. These results were obtained with standard groundwater flow models based on standard theory. Since the fluid density in these experiments was constant, no body forces were involved, and buoyancy in the conventional sense did not come into play. We therefore believe that the term “buoyancy reversal” is not quite appropriate to describe this phenomenon. What is actually observed is a reversal of the pressure gradient, so the appropriate term should be “pressure gradient reversal”.

Regardless of the terminology, we know from the field data presented by the author that the pressure gradient can reverse under certain conditions. We also know the theoretical conditions for reversal to occur, the key condition being that downward flow across the aquitard is equal to or greater than the hydraulic conductivity of the aquitard. This condition is clearly revealed by the 1D experiments. For 2D systems, the situation is more complex because flow is no longer forced vertically downward through the aquitard, but tends to be diverted laterally, forming a flow system. In any case, it is clear that for pressure gradient reversal to occur in an aquitard, a downward flux is necessary. Thus under natural conditions, a pressure gradient reversal can only occur underneath a groundwater recharge area.

This suggests that there may be potential applications of this concept in CO<sub>2</sub> storage. However, a concern would be that the required downward flow (recharge) would have to be balanced by corresponding discharge. A high flow rate across the aquitard also requires a high flow rate in the underlying aquifer. This may be contrary to the objectives of CO<sub>2</sub> sequestration over long periods of time, which would call for conditions of low mobility. The ideal conditions thus would be hydrostatic, but as the above examples have shown, hydrostatic conditions cannot produce a reversal of the pressure gradient.

Since the author has presented field data showing that the pressure gradient can reverse, studies should be conducted to investigate the conditions under which this occurs in the real world. The initial simulations should be done by means of a 2D cross-sectional flownet model. These simulations would be steady state due to the inherent limitations of flownet-type models. However, the effect of density variations should be considered.

If the 2D work is successful, subsequent work could focus on 3D simulations of CO<sub>2</sub> injection below an aquitard, combined with the injection of (possibly saline) water above the aquitard, as suggested by the author. These simulations should be done in transient state using a multiphase flow model. It should be kept in mind, however, that the idea of pumping saline water into the aquifer overlying the CO<sub>2</sub> storage aquifer would probably make sense in any case as a possible additional line of defense against leakage within a multi-barrier system, and the resulting pressure gradient reversal would be incidental. It should also be kept in mind that a system with a

denser fluid overlying a lighter fluid is basically unstable. This means that stability will be one of the aspects that would need to be investigated.

These simulations would give needed insights into the behaviour of the system under dynamic conditions. They would also provide answers to questions such as the long-term behaviour of the CO<sub>2</sub>, the length of time the water injection would have to be maintained, the mass loss of CO<sub>2</sub> from the system over the long term, the practicality of the scheme, the environmental impact, and the economics.

## References

- Bear, J., 1972. *Dynamics of Fluids in Porous Media*. American Elsevier, New York, N.Y.
- Chadwick, R.A., D.J. Noy, and S. Holloway, 2009. Flow processes and pressure evolution in aquifers during the injection of supercritical CO<sub>2</sub> as a greenhouse gas mitigation measure. *Petroleum Geoscience*, 15: 59-73.
- Freeze, R.A. and J.A. Cherry, 1979. *Groundwater*. Prentice-Hall, Englewood Cliffs, N.J.
- Frind, E.O., 1982. Simulation of long-term transient density-dependent transport in groundwater. *Advances in Water Resources*, 5(2): 73-88.
- Frind, E.O., 1982. Seawater intrusion in continuous coastal aquifer-aquitard systems, *Advances in Water Resources*, 5(2): 89-97.
- Frind, E.O., G.B. Matanga and J.A. Cherry, 1985. The dual formulation of flow for contaminant transport modeling: 2. The Borden Aquifer. *Water Resour. Res.* 21(2): 170-182.
- Frind, E.O. and G.B. Matanga, 1985. The dual formulation of flow for contaminant transport modeling: 1. Review of theory and accuracy aspects. *Water Resour. Res.* 21(2):159-169.
- Hubbert, M.K., 1940. The theory of groundwater motion. *J. Geol.* 48(8): 785-944.
- Kueper, B.H. and E.O. Frind, 1991. Two-phase flow in heterogeneous porous media: 2. Model application. *Water Resour. Res.* 27(6):1059-1070.
- Kueper, B.H. and E.O. Frind, 1991. Two-phase flow in heterogeneous porous media: 1. Model development. *Water Resour. Res.*, 27(6):1049-1057.

**Hydraulic head and pressure head profiles for multilayer system  
Case 1: Uniform material**

Aquifer

layer from top	thickness	Klayer
1	55	1
2	5	1
3	40	1
total thickn	100	

overall pressure gradient -0.8  
 overall hydraulic gradient 0.2  
 datum 100  
 harmonic mean Kharm 1  
 flux  $q = K_{harm} * \text{gradient}$  0.2  
 head drop over layer =  $q/K_{layer} * \text{thickness}$

head relative to head at top

elev	head drop	hydraulic head	pressure head
100	0	100	0
45	11.0000	89.0000	44.0000
40	1.0000	88.0000	48.0000
0	8.0000	80.0000	80.0000

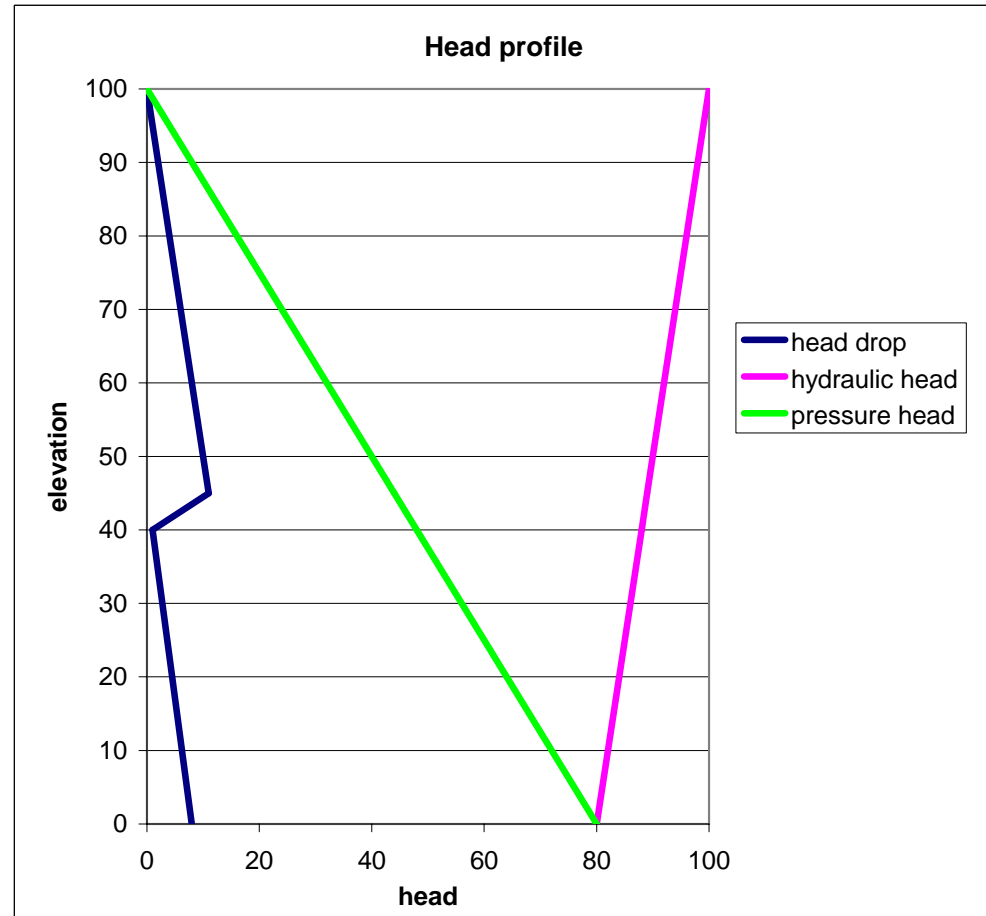


Figure 1: 1D column, downward flow, uniform material.

**Hydraulic head and pressure head profiles for multilayer system  
Case 2: Low-K layer, reversal of pressure gradient**

Aquifer

layer from top	thickness	Klayer
1	55	1
2	5	0.01
3	40	1
total thickn	100	

overall pressure gradient -0.8  
 overall hydraulic gradient 0.2  
 datum 100  
 harmonic mean Kharm 0.168067227  
 flux  $q = K_{harm} * \text{gradient}$  0.033613445  
 head drop over layer =  $q/K_{layer} * \text{thickness}$

head relative to head at top

elev	head drop	hydraulic head	pressure head
100	0	100	0
45	1.8487	98.1513	53.1513
40	16.8067	81.3445	41.3445
0	1.3445	80.0000	80.0000

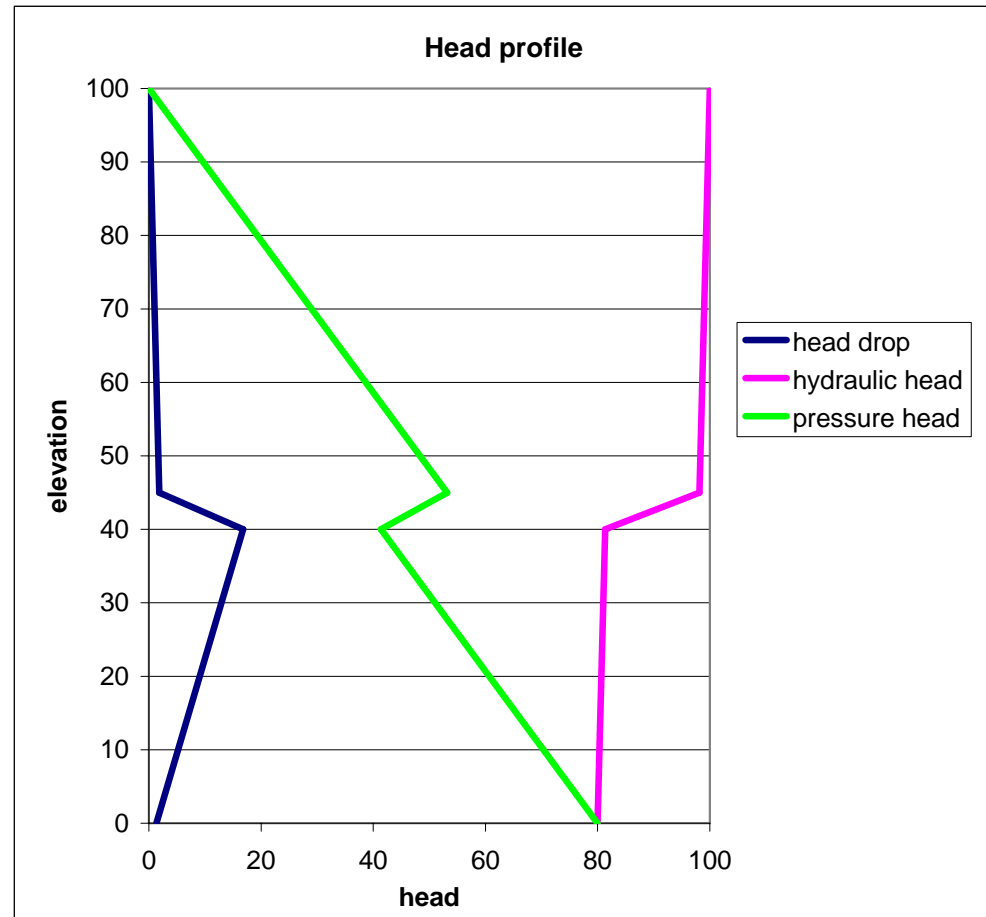


Figure 2: 1D column, downward flow,  $K_{aquitard}/K_{aquifer} = 10^{-2}$ , shows pressure gradient reversal.

**Hydraulic head and pressure head profiles for multilayer system**  
**Case 3: Critical case, gravity flow, flux =  $K_{layer}$**

Aquifer

layer from top	thickness	$K_{layer}$
1	55	1
2	5	0.15789
3	40	1
total thickn	100	

overall pressure gradient -0.8  
 overall hydraulic gradient 0.2  
 datum 100  
 harmonic mean  $K_{harm}$  0.789467763  
 flux  $q = K_{harm} * \text{gradient}$  0.157893553  
 head drop over layer =  $q/K_{layer} * \text{thickness}$

head relative to head at top

elev	head drop	hydraulic head	pressure head
100	0	100	0
45	8.6841	91.3159	46.3159
40	5.0001	86.3157	46.3157
0	6.3157	80.0000	80.0000

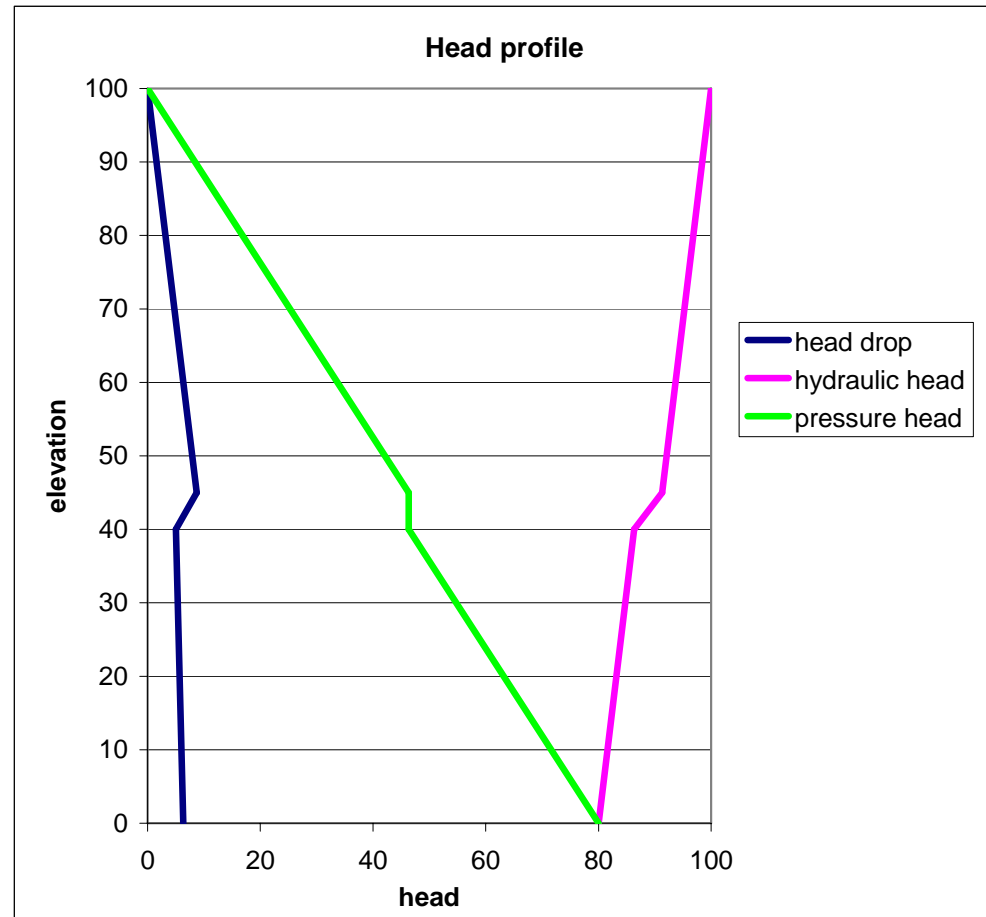


Figure 3: 1D column, downward flow,  $K_{aquitard} = \text{vertical flux} = \text{critical value for pressure gradient reversal}$ .

FLONET Pressure Inversion Test  
 Fixed head = 20m on right boundary, top surface recharge  
 Streamlines

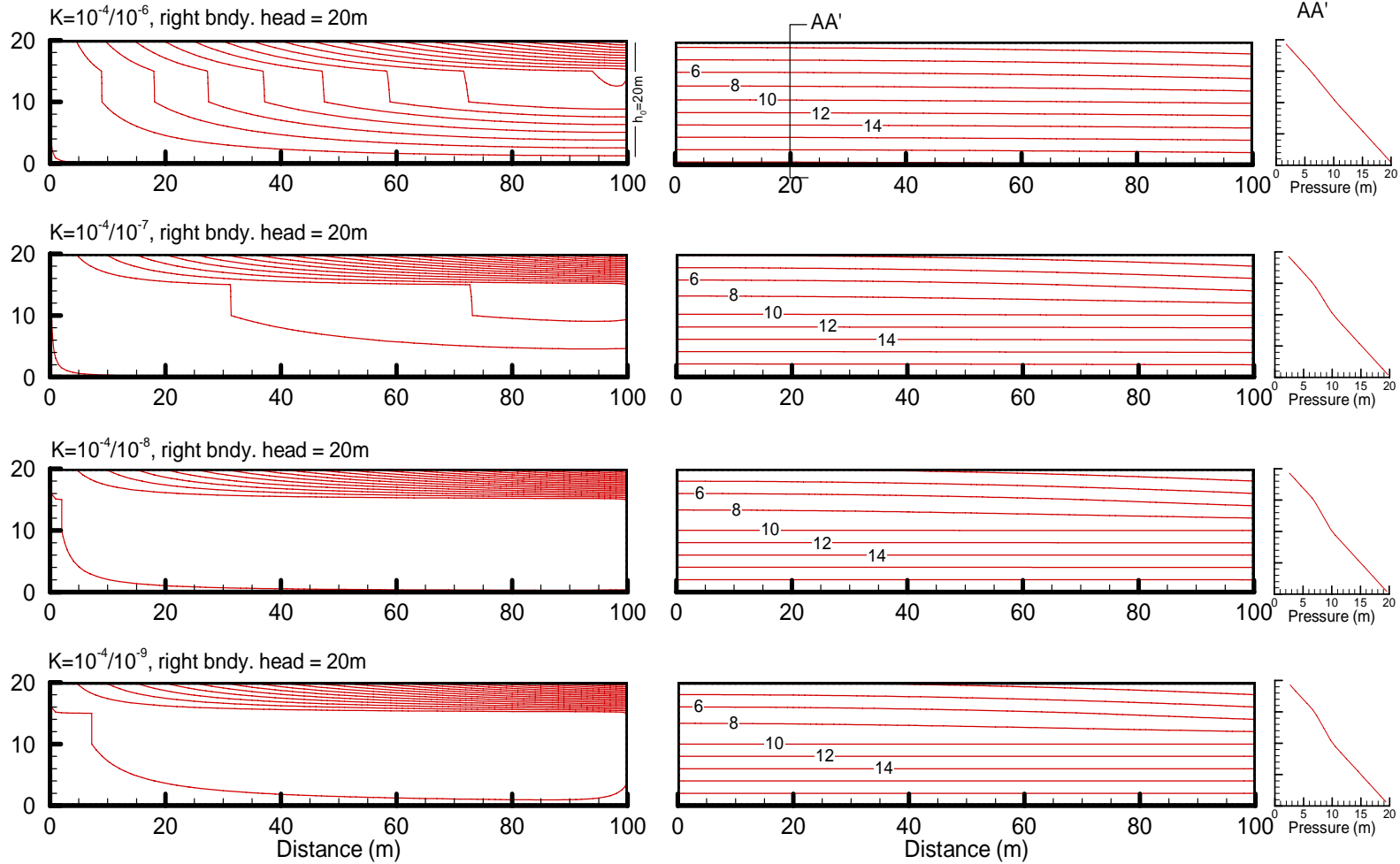
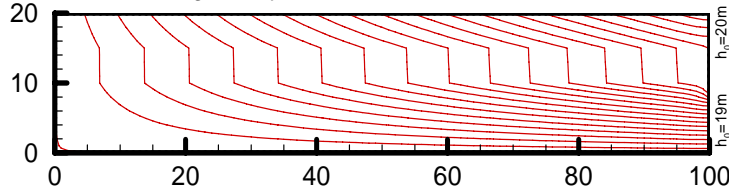


Figure 4: 2D aquifer/aquitard half flow system, specified recharge,  $K_{\text{aquitard}}/K_{\text{aquifer}} = 10^{-2}$  to  $10^{-5}$ , fixed uniform head on right boundary for all cases.

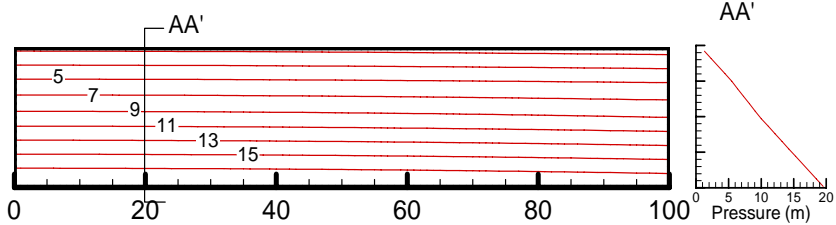
FLONET Pressure Gradient Inversion Test  
 Variable fixed heads on right boundary

Streamlines

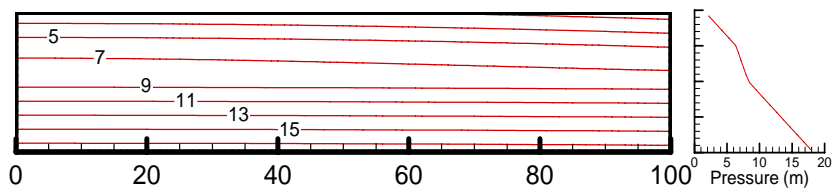
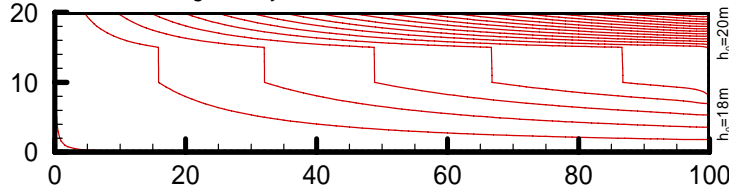
$K=10^{-4}/10^{-6}$ , right bndy. heads = 19 below, 20m above



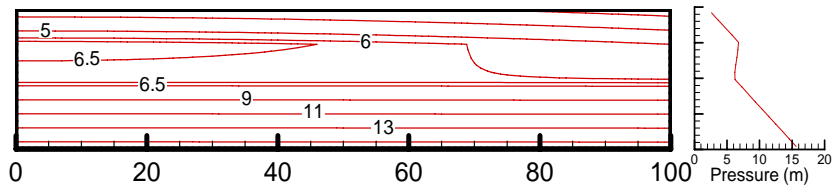
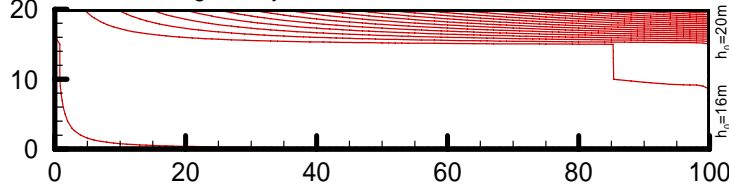
Pressure head (m)



$K=10^{-4}/10^{-7}$ , right bndy. heads = 18 below, 20m above



$K=10^{-4}/10^{-8}$ , right bndy. heads = 16 below, 20m above



$K=10^{-4}/10^{-9}$ , right bndy. heads = 14 below, 20m above

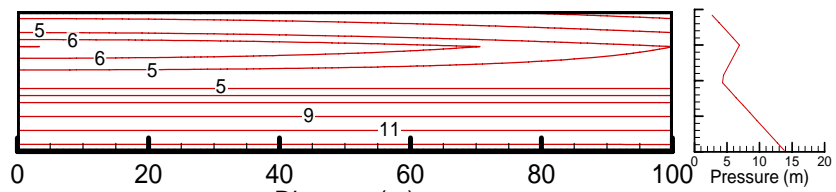
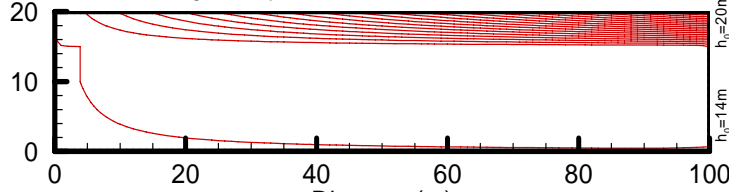


Figure 5: 2D aquifer/aquitard half flow system, specified recharge,  $K_{aquitard}/K_{aquifer} = 10^{-2}$  to  $10^{-5}$ , head at right boundary for lower aquifer decreased successively with decrease in  $K_{aquitard}$ .

Symmetry Boundary Model  
 1/2 cosine watertable: amplitude: +10/-10 m

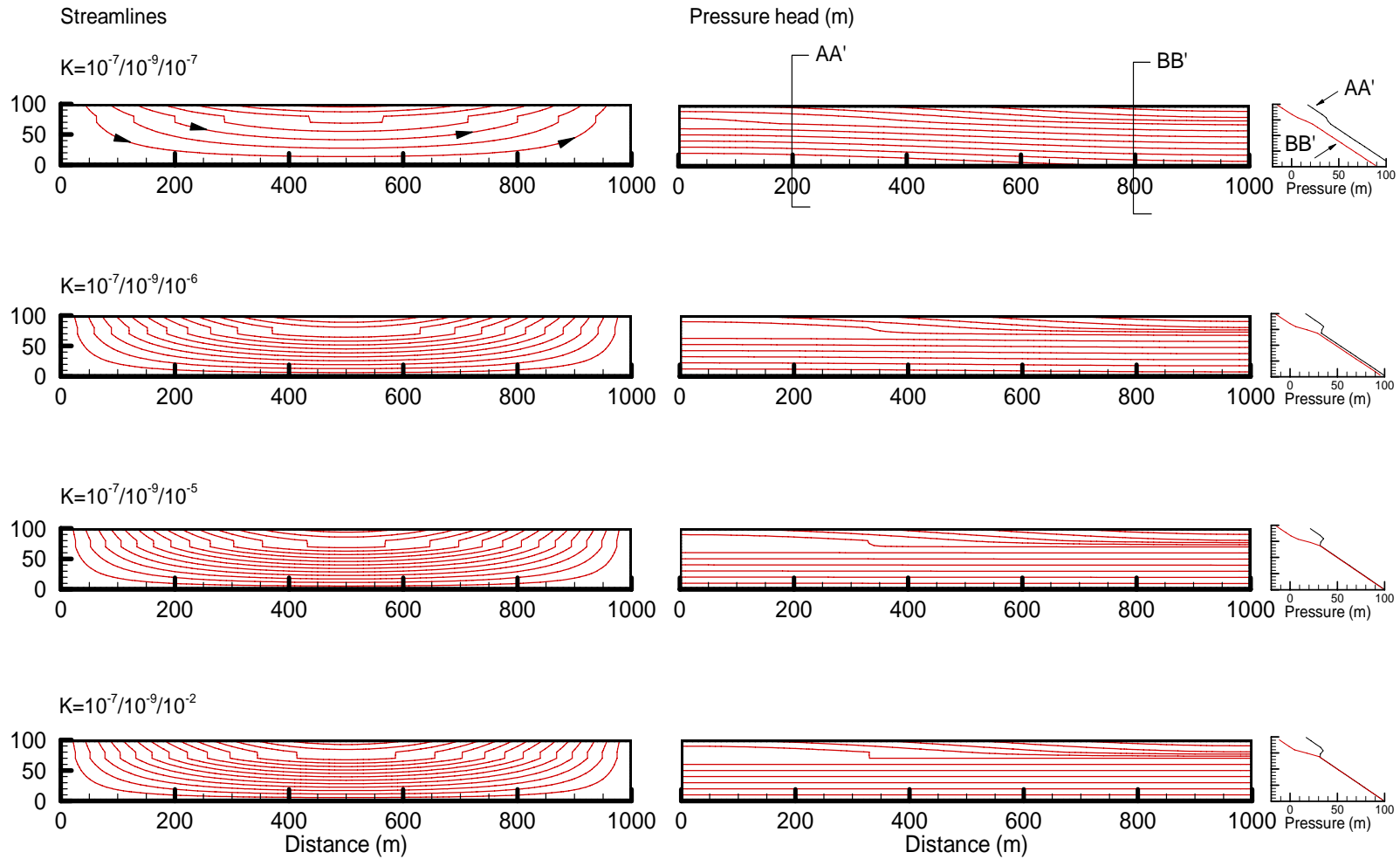


Figure 6: 2D aquifer/aquitard full flow system, symmetry boundaries left and right, specified watertable across top,  $K_{\text{aquitard}}/K_{\text{aquifer}}(\text{top}) = 10^{-2}$  for all cases, but  $K$  for lower aquifer increases from  $10^{-7}$  to  $10^{-2}$  toward bottom of figure.

## FLONET pressure gradient inversion test

watertable 1/2 cosine, Amp= $\pm 20$  m

$K$  aquitard =  $10^{-9}$  m/s

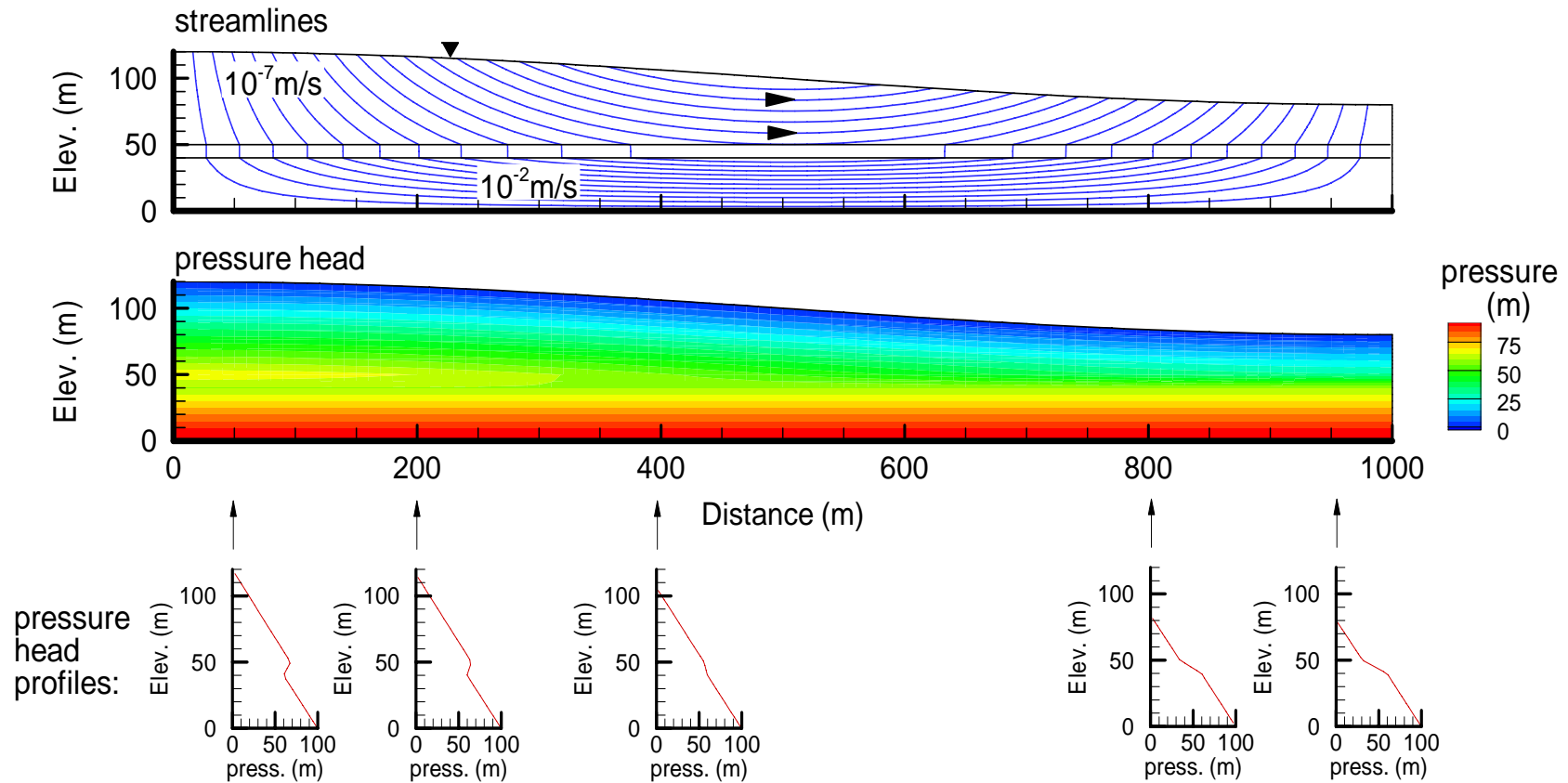


Figure 7: 2D aquifer/aquitard full flow system, symmetry boundaries left and right, specified watertable across top,  $K$ (upper aquifer) =  $10^{-7}$ ,  $K$ (aquitard) =  $10^{-9}$ ,  $K$ (lower aquifer) =  $10^{-2}$ .